An Efficient Field-Circuit Coupling Based on a Temporary Linearization of FE Electrical Machine Models

Enno Lange, François Henrotte, and Kay Hameyer

Institute of Electrical Machines-RWTH Aachen University, D-52062 Aachen, Germany

A field-circuit coupling method is presented, whose basic idea is to extract from the finite-element (FE) model a linearized lumped parameter representation of the electrical machines, to be used in the circuit simulator model of the power electronic supply. The dynamic coupled model of the complete drive obtained this way can be iterated over a limited period of time, with a time step adapted to the high frequency of electronic commutations. When the temporary representation of the machine has come, or is expected to have come under a given accuracy threshold, a new FE simulation is performed, a new set of lumped is generated and the process is repeated. This method allows decoupling the time constants of the field problem from that of the circuit problem, which is typically one or two orders of magnitude smaller. This yields a considerable saving of computation time with a controllable, at least *a posteriori*, loss of accuracy.

Index Terms—**Electric machines, energy-based linearization, field-circuit coupling, finite element methods.**

I. Introduction

VARIOUS approaches have been developed to simulate electrical machines driven by high frequency power converters. Whereas strong coupled approaches, e.g., [1] or [2], suffer from prohibitive computation times, weak coupled approaches, as proposed by [3], allow decoupling the time constants of each domain, which may differ by several orders of magnitude, making it possible to establish efficient and accurate numerical models.

This paper presents a method for coupling efficiently the computation time expensive finite-element (FE) model of an electrical machine with an external power electronics circuit. It is first explained how a linearized lumped parameter representation of an electrical machine seen from stator terminals can be systematically extracted from the FE model. This linearized representation is then inserted into the power electronics circuit equations of the converter and the aggregate circuit model is iterated in time until the linearization error is expected to have become too large with suspect to a predefined accuracy threshold. In contrast to [4], the lumped inductance matrix and the electromotive forces E_r are defined here on basis of energy-based arguments.

The field problem is thus temporarily represented in the circuit simulator equation by a set of lumped parameters, and time-consuming finite element simulations are used only to update the lumped parameters at a rate much slower than the rate of switching of the electronic components in the supply system. The overall computation time is thus considerably reduced.

The updating of the lumped parameters, is done either on a regularly basis (on the 20th circuit simulator iteration for instance), or on basis of an error estimator that triggers the generation of a new set of linearized data when the error of the present set exceeds a given threshold.

Manuscript received October 07, 2008. Current version published February 19, 2009. Corresponding author: E. Lange (e-mail: enno.lange@iem.rwth-aachen.de).

Color versions of one or more of the figures in this paper are available online at http://ieeexplore.ieee.org.

Digital Object Identifier 10.1109/TMAG.2009.2012585

II. Energy Balance in Magnetodynamics

The lumped parameters that represent an electrical machine in its supply power electronics circuit are the stator phase resistances and inductances, as well as the voltage E_r induced in the stator winding by the rotation of the machine. The approach presented in this paper consists in exploiting the FE Jacobian matrix of the magnetic system, which represents the first order linearization of the the nonlinear field equations around the operating point at time t. The lumped parameters as they are seen by the external circuit can be systematically extracted from it.

A relation between the field state variable (the vector potential $\mathbf{a}$) and the circuit state variables (the phase fluxes φ_r, $r = 1, \ldots, m$) is required for making this extraction. It is obtained on basis of energy considerations.

The energy balance of magnetodynamics systems can be represented by the diagram depicted in Fig. 1. It consists of an energy reservoir containing the magnetic energy Ψ_M of the system Ω and of a number of energy flows whose analytic expressions are given in the figure [5]. Stating power balance at the reservoir (variation of Ψ_M equals the sum of incoming flows) yields

$$\dot{\Psi}_M - \dot{W}_m = \int_\Omega \mathbf{j} \cdot \mathcal{L}_\mathbf{v} \mathbf{a} \tag{1}$$

where $\dot{W}_M$ is the power delivered by magnetic forces and $\mathcal{L}_\mathbf{v}\mathbf{a}$ denotes the material derivative of $\mathbf{a}$, i.e., a time derivative accounting for movement. On the other hand, power balance at the lower node of the energy diagram (sum of flow is zero) yields

$$\int_\Omega \mathbf{j} \cdot \mathcal{L}_\mathbf{v} \mathbf{a} = -\int_\Omega \frac{\mathbf{j}^2}{\sigma} - \int_\Omega \mathbf{j} \cdot \operatorname{grad} u. \tag{2}$$

The corresponding energy balance in terms of circuit quantities writes, respectively

$$\dot{\Psi}_M - \dot{W}_m = \sum_r I_r \dot{\varphi}_r \tag{3}$$

and

$$\sum_r I_r \dot{\varphi}_r = -\sum_r R_r I_r^2 + \sum_r I_r \Delta U_r \tag{4}$$

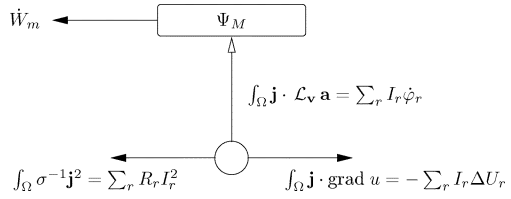

Fig. 1. Energy diagram of magnetodynamics and the expressions of the flows in both the field and the circuit representation.

where $\dot{\varphi}_r$ denotes the time derivative of the flux φ_r.

The principle of the identification between the field and the circuit variables relies now on the observation that the current density in stranded conductors can be written as

$$\mathbf{j} = \sum_r I_r \mathbf{w}_r \tag{5}$$

where the auxiliary field $\mathbf{w}_r$ can be regarded as the shape functions of the phase currents I_r. In 2-D, $\mathbf{w}_r = \pm(n_r/S_r)\mathbf{e}_z$ with n_r the number of turns and S_r the area of the coil domain, $+$ or $-$ sign being chosen according to the direction of the current. In 3-D, $\mathbf{w}_r$ is a vector field whose field lines follow the threads of the stranded coil.

Substituting (5) in the equations indicated in Fig. 1, one obtains readily

$$R_r = \int_\Omega \sigma^{-1} |\mathbf{w}_r|^2, \quad \Delta U_r = -\int_\Omega \mathbf{w}_r \cdot \mathrm{grad}\, u. \tag{6}$$

On the other hand, substituting (5) in

$$\int_\Omega \mathbf{j} \cdot \mathcal{L}_\mathbf{v} \mathbf{a} = \sum_r I_r \dot{\varphi}_r \tag{7}$$

yields

$$\dot{\varphi}_r = \int_\Omega \mathbf{w}_r \cdot \mathcal{L}_\mathbf{v} \mathbf{a}. \tag{8}$$

If the current distribution functions $\mathbf{w}_r$ are assumed not to depend on time (which is the case in coils), the sought mapping between $\mathbf{a}$ and φ_r is

$$\varphi_r = \int_\Omega \mathbf{w}_r \cdot \mathbf{a}. \tag{9}$$

In a mesh, this mapping between $\mathbf{a}$ and φ_r can be expressed by the rectangular matrix

$$\varphi_r = W_{ri} a_i \quad W_{ri} = \int_\Omega \mathbf{w}_r \cdot \boldsymbol{\alpha}_i \tag{10}$$

where $\boldsymbol{\alpha}_i$ are the shape functions of the $\mathbf{a}$ field, and a_i the corresponding coefficients.

III. Inductance Matrix

Let

$$M_{ij}(\mathbf{a}) a_j = b_i \tag{11}$$

with

$$b_i = \int_\Omega \mathbf{j} \cdot \boldsymbol{\alpha}_i = I_r \int_\Omega \mathbf{w}_r \cdot \boldsymbol{\alpha}_i = I_r W_{ir} \tag{12}$$

be the nonlinear FE magnetostatic equations describing the electrical machine under applied currents. Let I_r^* be the currents at time t, and $b_i^* = I_r^* W_{ir}$ the corresponding right-hand sides. Solving (11) with $b_i \equiv b_i^*$ and a fixed rotor angular position $\delta\Theta = 0$ gives a_j^* and a first order linearization around this particular solution writes

$$M_{ij}\left(a_j^* + \delta a_j\right) = M_{ij}\left(a_j^*\right) a_j^* + J_{ij}\left(a_j^*\right) \delta a_j = b_i^* + \delta b_i \tag{13}$$

with the Jacobian matrix $J_{ij} \equiv (\partial_{a_j} M_{ik}(a_j^*)) a_k^*$. Since $M_{ij}(a_j^*) a_j^* = b_i^*$, one has

$$J_{ij}\left(a_j^*\right) \delta a_j|_{\delta\Theta=0} = \delta b_i. \tag{14}$$

One can now repeatedly solve (14) with the right-hand sides $\delta b_i = \delta I_r W_{ir}$ obtained by perturbating one after the other m phase currents I_r and obtain m solution vectors for $\delta a_j|_{\delta\Theta=0}$. Since (14) is linear, the magnitude of the perturbations δI_r is arbitrary. One can so define by inspection the tangent inductance matrix L_{rs}^∂ of the electrical machine seen from terminals as

$$\begin{aligned} \delta\varphi_r|_{\delta\Theta=0} &= W_{rj} \delta a_j|_{\delta\Theta=0} \\ &= W_{rj} J_{ji}^{-1}\left(a_j^*\right) W_{is} \delta I_s \equiv L_{rs}^\partial \delta I_s \end{aligned} \tag{15}$$

with

$$L_{rs}^\partial = W_{rj} J_{ji}^{-1}\left(a_j^*\right) W_{is}. \tag{16}$$

Similarly, one can identify the secant inductance matrix L_{rs} and by solving (11) repeatedly with linearly independent phase currents I_r to obtain

$$\varphi_r = W_{rj} a_j = W_{rj} M_{ji}^{-1}\left(a_j^*\right) W_{is} I_s \equiv L_{rs} I_s \tag{17}$$

with

$$L_{rs} = W_{rj} M_{ji}^{-1}\left(a_j^*\right) W_{is}. \tag{18}$$

It is useful for these identifications to use a solver able of dealing efficiently with multiple right-hand sides.

IV. Motion Induced Voltage

One can now complement (15) to account for motion

$$\delta\varphi_r = L_{rs}^\partial \delta I_s + E_r \delta\Theta \tag{19}$$

with $E_r \equiv \partial_\Theta \varphi_r$. The direct computation of the Θ derivative would require to slightly shift the rotor, remesh, solve the FE problem, evaluate new fluxes and calculate a finite difference. In order to avoid this tedious process, one can again call on the energy principles. One has

$$E_r = \partial_\Theta \varphi_r = \partial_\Theta \partial_{I_r} \Psi_M = \partial_{I_r} \partial_\Theta \Psi_M = \partial_{I_r} T \tag{20}$$

where T is the torque. During the identification process described above, it is thus easy to calculate additionally the torque

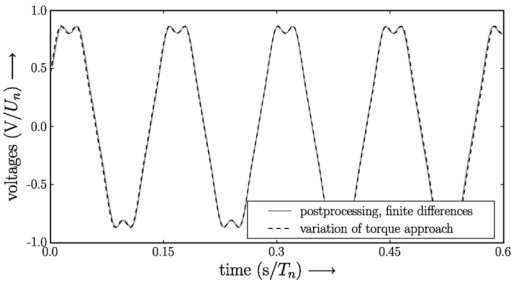

Fig. 2. Induced voltage at no load condition. Comparison between proposed variational approach and a calculation by post-processing with finite-differences.

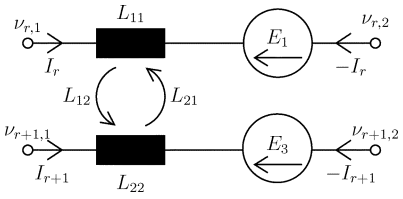

Fig. 3. Example of arbitrary lumped elements to be integrated within the circuit simulator.

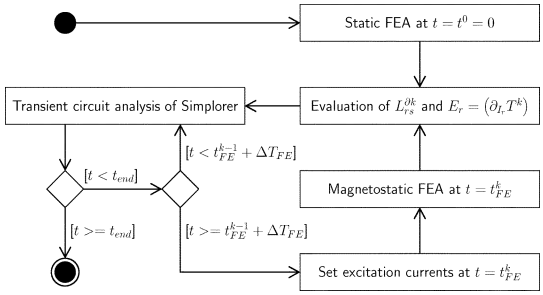

Fig. 4. Flowchart of the coupled simulation.

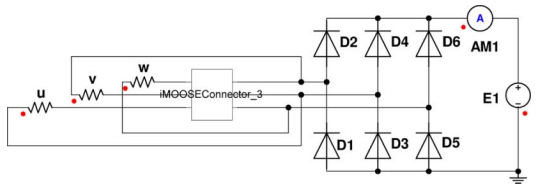

Fig. 5. Generator connected to a b6 rectifier working against a constant voltage source.

corresponding to the perturbed solutions $\delta a_j|_{\delta\Theta=0}$, and to evaluate the motion induced voltage E_r of each phase as the variation of the torque with the perturbation of the corresponding phase current I_r.

Beware however that, as the torque is a nonlinear function of the fields, the perturbations needs in this case be small. Because of the linearity of (14), one may scale the perturbation currents in (20) which yields

$$E_r = \frac{T\left(a_j^*\right) - T\left(a_j^* + \lambda\delta a_j|_{\delta\Theta=0}\right)}{\lambda\delta I_r} \quad \lambda = \kappa\frac{\left\|a_j^*\right\|_2}{\left\|\delta a_j\right\|_2}. \quad (21)$$

Herein, the scale factor is chosen between $0.01 \leq \kappa \leq 0.05$. Fig. 2 shows the induced voltage calculated by finite differences during a post-process and by the proposed energy based approach. Both are in fine accordance.

V. Circuit Representation of the FE Electrical Machine Model

Circuit simulators are usually based on the modified nodal analysis (MNA). The nonlinear equation systems are solved by the Newton–Raphson method. Depending on the choice of the state variable of the lumped parameter model, two representations of the FE-model are possible [6].

1) *State Variable:* Current, zeroth-order accurate.
If the current is the state variable, the voltage drop of the upper branch of the example depicted in Fig. 3 is

$$\begin{aligned}\nu_{r,1} - \nu_{r,2} &= \partial_t(L_{rs}I_s) \\ &= L^{\partial}{}_{rs}\delta I_s + (\partial_\Theta\varphi)\delta\Theta. \end{aligned} \quad (22)$$

2) *State Variable:* Flux, first-order accurate.
The current through the upper branch of Fig. 3 can be written as

$$\begin{aligned} I_r &= L_{rk}^{-1}\varphi_k + \partial_\varphi I\delta\varphi + \partial_\Theta I_r\delta\Theta \\ &= L_{rk}^{-1}\varphi_k + L^{\partial-1}{}_{rk}\delta\varphi + \partial_{\varphi_r}T\delta\Theta. \end{aligned} \quad (23)$$

Since the second representation requires the identification of both the secant and tangent inductance matrix, the current state based lumped parameter model has been implemented.

VI. Transient Coupling Scheme

The decoupled solution of the field and the circuit problems require a time stepping scheme to coordinate the interaction of the utilized FE-solver iMOOSE [7] and the circuit simulator *Simplorer* [8].

The basic scheme is shown in Fig. 4. The time step width ΔT_{FE} of the magnetostatic FE simulation is constant while the time step width of the circuit simulator is freely chosen by the simulator. The cosimulation starts with a static FE analysis to evaluate the initial lumped parameters, i.e., the tangent inductance matrix $L_{rs}^{\partial 0}$ and the motion induced voltages E_r^0. These values are incorporated into the equation system of the circuit simulator according to the MNA and the transient circuit analysis is started. If the global simulation time reaches $t \geq t_{\mathrm{FE}}^{k-1} + \Delta T_{\mathrm{FE}}$, the phase currents of the circuit simulator are transfered to the FE-solver and step k of the magnetostatic FE-system is calculated followed by the identification of the lumped parameters $L_{rs}^{\partial k}$ and E_r^k. Returning the new set of parameters to the circuit simulator the transient circuit analysis proceeds until $t \geq t_{\mathrm{end}}$ is reached.

The variable time step width of the circuit simulator allows it to adapt the step width according to the requirements of the high frequency switching components of the circuit domain.

VII. Application

The proposed field-circuit coupling has been applied to a three phase synchronous permanent magnet generator connected to a bridge-connected rectifier. The coupled problem has been simulated with both *Maxwell* [8] and the iMOOSE/*Simplorer* coupling described above. The topology of the system is shown in Fig. 5. The resistances are the phase resistances of the generator and "E1" is a constant voltage source. The block

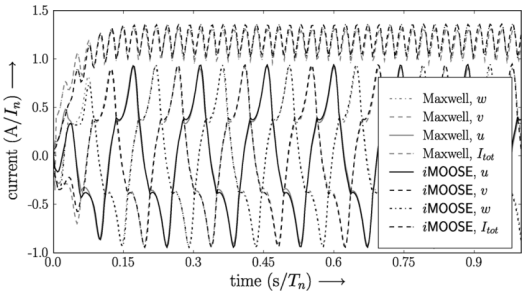

Fig. 6. Phase and total current forms at rated frequency $f_n = T_n^{-1}$.

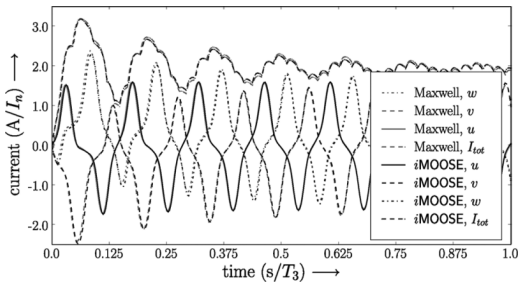

Fig. 7. Phase and total current forms at $f_3 = (25/3)T_n^{-1}$.

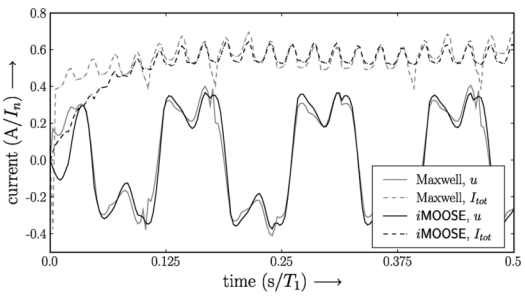

Fig. 8. Total and phase u current forms at $f_1 = (5/6)T_n^{-1}$.

"iMOOSEConnector_3" in Fig. 5 contains the lumped parameters L_{rs}^{∂} and E_r. All circuit parameters except those lumped parameters are being held constant throughout the simulation.

The comparison of the simulation results are shown in Fig. 6–Fig. 9. The rated point of operation can be seen in Fig. 6. The currents through phases u, v, and w as well as the total current I_{tot} are in good accordance except at the beginning of the simulation. Similar results can be observed at other points of operation, e.g., Fig. 7 (mechanical frequency $f_3 = (25/3)f_n$).

Being in good accordance at higher mechanical frequencies the results start to diverge at lower frequencies as can be seen in Fig. 8 (mechanical frequency of $f_1 = (5/6)f_n$). The divergence already observed at the beginning of the simulation in Fig. 6 becomes larger. Having a closer look at the terminal voltage depicted in Fig. 9, one recognizes overshoots at the peak values as well as around the singular switching points of the diodes in the calculation results of *Maxwell*. This behavior lacks a physical explanation and indicates an inaccurate zero crossing detection of the diodes.

The simulation results of the proposed lumped parameter coupled method are in good accordance with the simulation

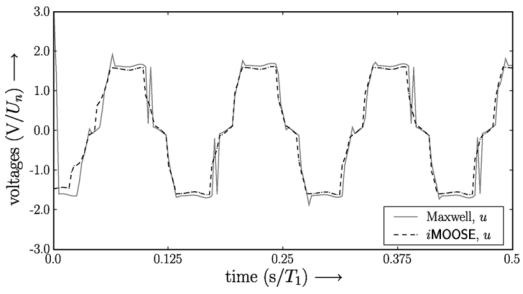

Fig. 9. Terminal voltage of phase u at $f_1 = (5/6)T_n^{-1}$.

results of *Maxwell* with a significant time saving of approximately 25%.

VIII. Conclusion

In this paper, an efficient field circuit coupling based on a temporary linearization of the FE electrical machine model is presented. The linearization of the FE model is derived from the energy flow in the electrical machine with a consistent mapping between the state variables, i.e., vector potential and flux. The lumped parameters are extracted and incorporated into a circuit simulator. The proposed method has been applied to a permanent magnet generator and the simulation results have been compared to a commercial FE-software package and validated. The proposed method turns out also to be more agile in dealing accurately with zero crossing detection.

The proposed method saves computation time by reducing costly FE-simulations to a minimum. It is applicable to two and three dimensional problems. A further step will be the implementation of an *a priori* linearization error estimator in order to reduce the number of parameter identifications, thus reducing further the overall computational time. Finally, an experimental setup for the experimental validation of the coupling is under construction [9].

References

[1] T. Dreher and G. Meunier, "3D line current model of coils and external circuits," *IEEE Trans. Magn.*, vol. 31, no. 3, pp. 1853–1856, May 1995.

[2] A. Canova, M. Ottella, and D. Rodger, "Coupled field-circuit approach to 3D FEM analysis of electromechanical devices," in *Proc. 9th Int. Conf. Elect. Mach. Drives*, 1999, pp. 71–75.

[3] P. Zhou, D. Lin, W. N. Fu, B. Ionescu, and Z. J. Cendes, "A general cosimulation approach for coupled field-circuit problems," *IEEE Trans. Magn.*, vol. 42, no. 4, pp. 1051–1054, Apr. 2006.

[4] S. Kanerva, S. Seman, and A. Arkkio, "Inductance model for coupling finite element analysis with circuit simulation," *IEEE Trans. Magn.*, vol. 41, no. 5, pp. 1620–1623, May 2005.

[5] F. Henrotte and K. Hameyer, "The structure of electromagnetic energy flows in continuous media," *IEEE Trans. Magn.*, vol. 42, no. 4, pp. 903–906, Apr. 2006.

[6] N. A. Demerdash and T. W. Nehl, "Electric machinery parameters and torques by current and energy perturbations from field computations—Part I: Theory and formulation," *IEEE Trans. Energy Conv.*, vol. 14, no. 4, pp. 1507–1513, Dec. 1999.

[7] G. Arians, T. Bauer, C. Kaehler, W. Mai, C. Monzel, D. van Riesen, and C. Schlensok, "Innovative Modern Object-Oriented Solving Environment—iMOOSE," 2008. [Online]. Available: http://www.imoose.de

[8] Ansoft Corporation, Canonsburg, PA, "Maxwell/Simplorer," 2008. [Online]. Available: http://www.ansoft.com

[9] M. van der Giet, E. Lange, and K. Hameyer, "Test case for the verification and benchmarking of coupled electromagnetic field and circuit simulation," in *Proc. XX Symp. Electromagn. Phenomena Nonlinear Circuits*, Jul. 2008, pp. 39–40.